AGU PUBLICATIONS

Water Resources Research

RESEARCH ARTICLE
10.1002/2013WR014950

Key Points:
- Often, the sensible heat flux is estimated using the Ohm's law analogy, HOhm
- HOhm involves the canopy parameter, kB^{-1}, that is difficult to interpret
- A method is proposed that does not involve kB^{-1}; it is an alternative to HOhm

Correspondence to:
F. Castellví,
f-castellvi@macs.udl.cat

Citation:
Castellví, F., P. Gavilán, and M. P. González-Dugo (2014), Combining the bulk transfer formulation and surface renewal analysis for estimating the sensible heat flux without involving the parameter kB^{-1}, *Water Resour. Res.*, *50*, 8179–8190, doi:10.1002/2013WR014950.

Received 25 OCT 2013
Accepted 25 SEP 2014
Accepted article online 30 SEP 2014
Published online 21 OCT 2014

Combining the bulk transfer formulation and surface renewal analysis for estimating the sensible heat flux without involving the parameter kB^{-1}

F. Castellví[1], P. Gavilán[2], and M. P. González-Dugo[2]

[1]Department of Environmental and Soil Sciences, University of Lleida, Lleida, Spain, [2]IFAPA, Centro Alameda del Obispo, Córdoba, Spain

Abstract The single-source bulk transfer formulation (based on the Monin-Obukhov Similarity Theory, MOST) has been used to estimate the sensible heat flux, *H*, in the framework of remote sensing over homogeneous surfaces (H_{MOST}). The latter involves the canopy parameter, kB^{-1}, which is difficult to parameterize. Over short and dense grass at a site influenced by regional advection of sensible heat flux, H_{MOST} with $kB^{-1} = 2$ (i.e., the value recommended) correlated strongly with the *H* measured using the Eddy Covariance, EC, method, H_{EC}. However, it overestimated H_{EC} by 50% under stable conditions for samples showing a local air temperature gradient larger than the measurement error, 0.4 km^{-1}. Combining MOST and Surface Renewal analysis, three methods of estimating *H* that avoid kB^{-1} dependency have been derived. These new expressions explain the variability of *H* versus $u_*\left(T_c - T_{(z)}\right)$, where u_* is the friction velocity, T_c is the radiometric surface temperature, and $T_{(z)}$ is the air temperature at height, z. At two measurement heights, the three methods performed excellently. One of the methods developed required the same readily/commonly available inputs as H_{MOST} due to the fact that the ratio between $\left(T_c - T_{(z)}\right)$ and the ramp amplitude was found fairly constant under stable and unstable cases. Over homogeneous canopies, at a site influenced by regional advection of sensible heat flux, the methods proposed are an alternative to the traditional bulk transfer method because they are reliable, exempt of calibration against the EC method, and are comparable or identical in cost of application. It is suggested that the methodology may be useful over bare soil and sparse vegetation.

1. Introduction

Many remote sensing studies over homogeneous surfaces have used the single-source bulk transfer formulation (based on Monin-Obukhov Similarity Theory, MOST) to estimate the sensible heat flux, *H*, as follows [*Brutsaert*, 1982]

$$H = \rho C_p \frac{T_c - T_{(z)}}{r_{ah(z)}} \quad (1)$$

where ρ and C_p are the air density and specific heat capacity at constant pressure, respectively, $z = (Z - d)$ is a reference height, *Z* and *d* are the measurement height above the ground and the zero-plane displacement, respectively, T_c is the radiometric surface temperature, $T_{(z)}$ is the air temperature, and $r_{ah(z)}$ is the aerodynamic resistance to heat transfer. Because the roughness length for momentum, z_{0m}, exceeds the roughness length for heat transfer, z_{0h}, $r_{ah(z)}$ can be expressed as, $r_{ah(z)} = r_{ahm(z)} + r_{ex}$, where $r_{ahm(z)}$ is the aerodynamic resistance for momentum transfer and r_{ex} is an excess of resistance, $r_{ex} = \frac{kB^{-1}}{ku_*}$ [*k* is the von Kármán constant, u_* is the friction velocity, and $kB^{-1} = \ln\left(\frac{z_{0m}}{z_{0h}}\right)$]. In equation (1), it is assumed that the surface is isothermal and, therefore, $T_c \approx T_{(z_{0h})}$. However, while z_{0m} is a canopy parameter that can be determined using the wind log-law, z_{0h} is not clearly defined because $T_{(z_{0h})}$ cannot be measured (i.e., even over homogeneous canopies the assumption that $T_c = T_{(z_{0h})}$ is strict and should be taken, in general, as an approximation [*Choudhury et al.*, 1986; *Boulet et al.*, 2012; *Crago and Qualls*, 2014]), and the profile predicted by MOST does not hold within the roughness sublayer [*Graefe*, 2004; *Harman and Finnigan*, 2007, 2008; *Belcher et al.*, 2012]. Subsequently, parameterization of the parameter kB^{-1} has been the subject of intensive research for several decades and the amount of work published on this topic is enormous [*Owen and Thomson*, 1963; *Chamberlain*, 1968; *Thom*, 1975; *Garratt and Francey*, 1978; *Brutsaert*, 1982; *Kustas et al.*, 1989; *Kalma and Jupp*, 1990; *Duynkerke*, 1992; *McNaughton and*

Van den Hurk, 1995; *Verhoef et al*., 1997; *Chehbouni et al*., 1996; *Troufleau et al*., 1997; *L'Homme et al*., 2000; *Colaizzi et al*., 2004; *Mahrt and Vickers*, 2004; *Matsushima*, 2005; *Kustas et al*., 2007; *Yang et al*., 2008; *Liu et al*., 2006; *Haverd et al*., 2010; *Boulet et al*., 2012; *Hong et al*., 2012; *Crago and Qualls*, 2014] (to mention a few).

It is, therefore, of interest to develop simple alternative procedures to equation (1) for estimating H (i.e., using T_c) without involving the parameter kB^{-1} and minimizing input requirements to facilitate its implementation. The latter may be achieved by using the Surface Renewal, SR, method because it is not based on MOST and avoids the inherent complexity of detailed multilayered formulation in the canopy [*Paw U et al*., 1995]. Taking measurements at a single height above the canopy, the SR method estimates the surface flux of a scalar based on the role of coherent structures which can be abstracted as follows: a fresh air parcel traveling in the bulk of the flow suddenly descends to the ground and, while connected to the sources, becomes gradually enriched by a scalar. After a given period, the parcel is, by continuity, replaced and ejected upward. The latter represents an injection of scalar into the bulk of the flow which can be identified by a regular ramp-like shape observed in the scalar concentration time series (recorded at high frequency) measured above the surface. The SR method has been successfully employed over various canopies to estimate H from the air temperature, which is typically measured at between 8 and 20 Hz in either the roughness or inertial sublayers [*Paw U et al*., 1995; *Snyder et al*., 1996; *Castellví*, 2004, 2013; *Castellví and Snyder*, 2009; *Shapland et al*., 2012; *French et al.,* 2012]. Using thermal infrared (IR) imagery with a large field of view, spatial trends in T_c along transects in direction of the wind have been observed. This feature has been related to the role of coherent structures [*Derksen*, 1974; *Schols et al*., 1985; *Ballard et al*., 2004; *Vogt*, 2008; *Christen et al*., 2012; *Garai and Kleissl*, 2011; *Garai et al*., 2013]. In relation to the framework of remote sensing to estimate H, *Garai and Kleissl* [2011] have recently pioneered the application of the earlier SR method to estimate H from measurements of T_c using a thermal IR camera operating at 1 Hz. Over a homogeneous surface, this new methodology appears to be suitable when convection dominates the turbulence in the atmospheric surface layer. However, an IR camera is expensive and a wide field of view is required to cover the dimensions of the coherent structures (i.e., a tall mast must be available).

The aim of this work was to derive an SR-based equation to estimate H involving low-frequency, e.g., half hourly, measurements of T_c. It thus avoids kB^{-1} as input or acquisition of expensive thermal cameras. It is shown that the mean (half hourly) ramp amplitude, $A_{(z)}$ (observed in a series of $T_{(z)}$ measured at high frequency), and $(T_c - T_{(z)})$ may be related. This finding allows derivation of three SR-based methods to estimate H without the need to estimate the ramp period, τ. These SR methods have been applied using the ramp models proposed by *Van Atta* [1977] and *Chen et al*. [1997a]. Over a homogeneous, dense and short canopy, the performance of equation (1) and the proposed methods were compared against the sensible heat flux measured using the Eddy Covariance, EC, method, H_{EC}. Thus, equation (1) was assumed to be independent (i.e., did not require calibration) because such a canopy minimizes the uncertainty in measuring T_c and in estimating canopy parameters, such as d, z_{0m}, and kB^{-1}, that are required to determine $r_{ah(z)}$ [*Thom*, 1975; *Brutsaert*, 1982; *Liu et al*., 2006]

$$r_{ah(z)} = \frac{1}{ku_*}\left(\ln\left(\frac{z}{z_{0m}}\right) + kB^{-1} - \Psi_{h(z/L)} + \Psi_{h(z_{0h}/L)}\right) \tag{2}$$

where L is the Obukhov length and $\left(\Psi_{h(z/L)} - \Psi_{h(z_{0h}/L)}\right)$ is defined as, $\left(\Psi_{h(z/L)} - \Psi_{h(z_{0h}/L)}\right) = \int_{\frac{z_{0h}}{L}}^{z/L}\left(1-\phi_h(x)\right)\frac{dx}{x}$,

where $\phi_{h(z/L)}$ is the stability correction function for heat transfer. The experiment was carried out in summer at a site where positive H_{EC} was rarely observed. Thus, this study focuses mainly on stable cases.

2. Theory

In the inertial sublayer, provided that the horizontal mean wind speed and the air temperature measured at high frequency are available at one height, H can be estimated as [*Castellví*, 2013]

$$H = \rho C p\sqrt{\frac{K_h}{\pi}\frac{A^2}{\tau}} \tag{3}$$

where H and A have the same sign, and K_h is the eddy diffusivity for heat transfer. In equation (3), K_h can be determined as $K_h = nK_{hMOST}$, where n is a coefficient and K_{hMOST} is the K_h predicted by MOST,

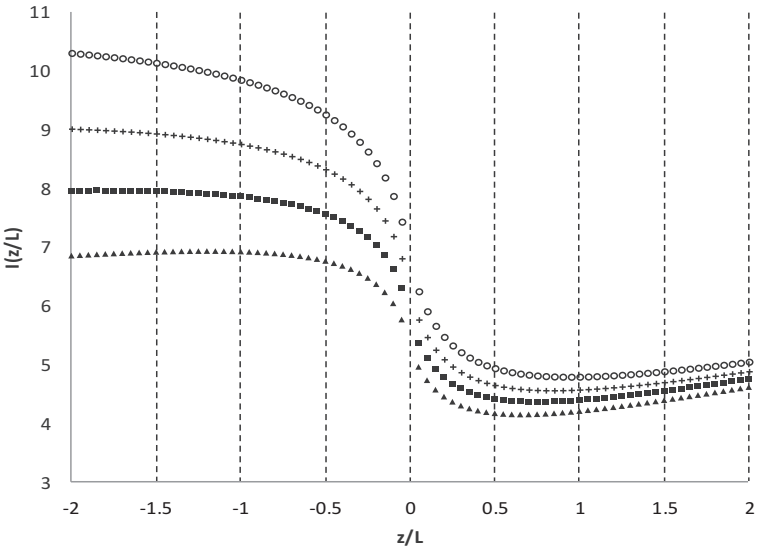

Figure 1. The function $I_{(z/L)}$ versus z/L determined over a hypothetical homogeneous canopy taking measurements at $Z = 0.9$ m (solid triangle) and at $Z = 1.5$ m (solid square) when the canopy height, h, is $h = 0.15$ m, and at $Z = 2.5$ m (plus) and at $Z = 3$ m (open circle) for $h = 0.5$ m.

$K_{hMOST} = kzu_* \phi_h^{-1}(z/L)$. When $\frac{A^2}{\tau}$ is determined using the method proposed by *Van Atta* [1977], VA, for the shortest time lags and by *Chen et al*. [1997a], Chen, values of the coefficient n is 1 and 2, respectively [*Castellví*, 2013]. The difference between the ramp models is the following. The VA ramp model allows for a quiescent time period, L_q, and neglects the microfront time period, L_m. Thus, $(\tau - L_q)$ is the warming time period. However, the Chen ramp model assumes that $L_q = 0$ and takes L_m into account. Thus, $(\tau - L_m)$ is the warming time period. Irrespective of which ramp model is used, the ramp amplitude determined is similar. However, the coefficient n is different because the ramp period determined using Chen's model is about twice that of VA's model [*Chen et al*., 1997a].

2.1. Relating $(T_c - T_{(z)})$ and $A_{(z)}$ Above the Canopy

Combining equations (1)–(3), $kB^{-1} = \ln\left(\frac{z_{0m}}{z_{0h}}\right)$ and $K_h = nK_{hMOST}$, the difference $(T_c - T_{(z)})$ can be expressed as

$$(T_c - T_{(z)}) = s_{(z)} A_{(z)} \text{ where } s_{(z)} = \left(\frac{nz}{\pi k \tau u_*}\right)^{1/2} I_{(z/L)} \text{ and } I_{(z/L)} = \frac{1}{\phi_h^{1/2}{}_{(z/L)}} \int_{z_{0h}/L}^{z/L} \phi_{h(x)} \frac{dx}{x} \quad (4)$$

A nonzero mean local vertical gradient, $\frac{\partial T_{(z)}}{\partial z}$, is required to observe ramps in air temperature time series [*Holzer and Siggia*, 1994], and while $A_{(z)}$ is related with $\partial T_{(z)}$, τ is mainly dependent on the transfer of momentum to the ground. Thus, $\frac{1}{\tau}$ is expected to be related with $\frac{u}{z}$ or $\frac{u_*}{z}$ [*Paw U et al*., 1992; *Chen et al*., 1997b; *Castellví et al*., 2002; *Finnigan et al*., 2009; *Shapland et al*., 2012]. Therefore, for a given measurement height, the parameter $s_{(z)}$ mainly depends on the stability conditions. Above two homogeneous canopies with heights, $h = 0.1$ m and $h = 0.5$ m, Figure 1 shows $I_{(z/L)}$ for two typical measurement heights at which d, z_{0m}, and kB^{-1} were determined as $d = 2/3h$, $z_{0m} = 0.12h$, and $kB^{-1} = 2$ [*Garratt and Francey*, 1978; *Brutsaert*, 1982]. Figure 1 shows that $I_{(z/L)}$ is steep near neutral conditions ($-0.25 \leq z/L \leq 0.25$), and fairly constant outside this range, especially for stable cases. Overall, for a given range of stable and unstable conditions, one may expect $s_{(z)}$ to remain fairly constant at a fixed height.

2.2. Estimating H

The mean air temperature can be expressed as [*Castellví and Snyder*, 2009]

$$T_{(z)} = fA_{(z)} + T_b \quad (5)$$

where $f = \frac{1}{2}\frac{(\tau - L_q)}{\tau}$ or $f = \frac{1}{2}$ using the VA or Chen ramp models, respectively, and T_b is the air temperature at the top of the coherent structure. Appendix A shows that irrespective of which ramp model is employed, the profile of the ramp amplitude can be expressed as

$$A_{(z)} = a_1 z^{a_2} \tag{6}$$

where a_1 and a_2 are the two coefficients. The sign of a_1 and $A_{(z)}$ is the same and the sign of a_2 is negative. The following equation, equation (7), is obtained by differentiating equations (4) and (5) with respect to z

$$\frac{\partial s_{(z)}}{\partial z} A_{(z)} + s_{(z)} \frac{\partial A_{(z)}}{\partial z} + f \frac{\partial A_{(z)}}{\partial z} = 0 \tag{7}$$

with the boundary condition invoked in equation (1) at ground level, $T_c = T_{(z_{0h})}$, and denoting A_0 as, $A_0 = A_{(z_{0h})}$, the solution of equation (7) is

$$1 + \frac{s_{(z)}}{f} = \frac{A_0}{A_{(z)}} = \left(\frac{z_{0h}}{z}\right)^{a_2} \tag{8}$$

Provided that the air temperature is available at two heights, combining equations (4), (6), and (8), the coefficient a_2 can be determined as

$$a_2 = \frac{\ln\left(\frac{T_c - T_{(z_2)}}{T_c - T_{(z_1)}}\right) + \ln\left(\frac{l_{(z_1/L)}}{l_{(z_2/L)}}\right)}{\ln\left(\frac{z_2}{z_1}\right)} - 0.5 \tag{9}$$

with the flux-gradient relationship $H = -\rho C_p K_h \frac{\partial T_{(z)}}{\partial z}$, implementing equations (4)–(6), the sensible heat flux is expressed as

$$H = -\rho C_p \left(k u_* \phi_h^{-1}{}_{(z/L)}\right)\left(T_c - T_{(z)}\right)\left(\frac{nfa_2}{s_{(z)}}\right) \tag{10}$$

Despite the fact that equation (10) does not involve the parameter kB^{-1}, the error in determining the coefficient a_2 may be large when $\frac{\partial T_{(z)}}{\partial z}$ is small (i.e., when $\left(T_{(z_2)} - T_{(z_1)}\right)$ falls within the range of measurement error). In practice, it is desirable to avoid installing tall masts. Thus, the ratio z_2/z_1 is, typically, $z_2/z_1 \leq 2$, and the error may be significant. To bypass this shortcoming, we used the following SR-based expression for estimating the sensible heat flux [*Castellví et al.*, 2002; *Castellví*, 2004]

$$H_{SR} = \rho C_p k \beta \phi_h^{-1}{}_{(z/L)} u_* A_{(z)} \tag{11}$$

where β is a semiempirical parameter. Under near-neutral and unstable conditions, β was found to remain fairly constant over homogeneous and heterogeneous canopies. In practice, regardless of the stability conditions, it can be estimated as $\beta = \left(\frac{\lambda}{\pi k} \phi_{h(z/L)}\right)^{1/2}$, where λ can be set to $\lambda = 0.40$, $\lambda = 0.54$, and $\lambda = 0.70$ over bare soil, short, and tall (forest) homogeneous canopies, respectively [*Chen et al.*, 1997b; *Castellví*, 2004]. Combining equations (4) and (11), and comparing with equation (10), $\beta = -nfa_2$. Under convective and close to neutral conditions, $\frac{\partial T_{(z)}}{\partial z}$ is small and because for such cases β and $s_{(z)}$ are expected to remain fairly constant, it may be useful to estimate H using the following approach:

$$H = -\rho C_p k \alpha_{(z)} \phi_h^{-1}{}_{(z/L)} u_* \left(T_c - T_{(z)}\right) \tag{12}$$

where $\alpha_{(z)} = \frac{\beta}{s_{(z)}}$. Because λ values were obtained using Chen's model, it is recommended to determine $\alpha_{(z)}$.

3. Materials and Methods

3.1. The Field Experiment

From 10 July 2009 to 28 September 2009, an experiment was conducted in the Guadalquivir Valley at the Agricultural Training and Research Centre of Alameda del Obispo (37°51′N, 4°51′W) in a plot (190 m in the mean streamwise direction, N-W, × 150 m = 2.85 Ha) of sprinkler-irrigated grass (*Festuca arundinacea*, 0.15 m tall). The surroundings mainly consisted of short irrigated crops and bare soil. Prior to the campaign, from 1 to 9 July (hereafter referred to as period of comparison), two identical EC systems to determine H_{EC} were deployed 145 m from the edge (in the prevailing wind direction) at $Z = 1.5$ m and 1.5 m apart. Each EC system consisted of a triaxial sonic anemometer (CSAT3 Campbell Scientific, Inc., Csi) and a fine-wire thermocouple (12.7 μm diameter, FW05 Csi). The air temperature and the three wind speed components were recorded at 20 Hz using a data logger CR5000 (Csi). The period of comparison was used to determine differences in H_{EC} and in the half-hourly air temperature. On 10 July, one EC system was deployed at $Z = 0.9$ m while the other system remained at Z = 1.5 m, and the half-hourly radiometric surface

temperature was measured using an IRTS-P sensor (Csi and Apogee Instruments, Inc.) deployed at $Z = 5.2$ m and nadir looking. Thus, during the campaign, the H estimates using equations (1), (10), and (12) were determined at two heights.

The weather observed was mainly characterized by clear sky days, high temperatures (at $Z = 1.5$ m, the mean was 27.5°C and range between 15°C and 41°C), light winds (the horizontal half-hourly mean wind speed at $Z = 1.5$ m was 1.8 m s^{-1}), and the measured sensible heat flux was positive mostly from dawn to about 14.00 h (GMT), though for some days H_{EC} was always negative. Such weather is a typical of the climate of the Guadalquivir Valley [*Hernández-Ceballos et al*., 2013].

3.2. The Data Sets and the H Taken as a Reference for Comparison

The instruments were covered for protection when storms were forecast (according to the National Weather Forecasting Centre) and during irrigation (scheduled every 3 days). The data sets also excluded samples with $u_* \leq 0.1$ m/s to ensure accurate measurement of the sensible heat flux [*Steeneveld et al*., 2006] and samples with a fetch of <80 m, to avoid flow distortion and flux footprints from bare soil and from the path used to access the instrumentation. Finally, samples were excluded if $\left(T_c - T_{(z)}\right)$ and H_{EC} had different signs so as to not distort the comparison of the H estimates versus H_{EC}. Regardless of the measurement height and for $u_* \geq 0.1$ m/s, the counter-gradient problem was observed in 102 samples, all collected near-neutral cases. The H_{EC} was in the range -31 W $m^{-2} \leq H_{EC} \leq 29$ W m^{-2}. Because, in practice, H_{EC} is not known, it is worth mentioning that this shortcoming (i.e., the counter-gradient issue is a problem inherent in equations (1), (10), and (12)) can be addressed by determining the sign of the third-order structure function that is the opposite to H_{EC}. Once these samples are identified, H cannot be estimated.

During the period of comparison, the maximum difference (absolute value) and the mean difference in the half-hourly fine-wire thermocouple measurements were 0.23 and 0.04 K, respectively. The slope and intercept of the linear regression analysis comparing the half-hourly air temperature using different thermocouples were 1.00 and 0.00 K, respectively, and the coefficient of determination, R^2, was $R^2 = 0.99$. Therefore, a data set, referred to as data set_1, excluded the samples with differences in $|T_{(Z=1.5\ m)} - T_{(Z=0.9\ m)}| < 0.25$ K to avoid uncertainties in equation (9). Another data set, data set_2, was formed with samples having $|T_{(Z=1.5\ m)} - T_{(Z=0.9\ m)}| < 0.25$ K. For data set_1, because only 27 samples show H_{EC} positive, they were removed (i.e., the data set was too short). With regard to the H_{EC} measured during the period of comparison, the slope, intercept, and coefficient R^2 of the linear regression analysis were 1.015, 0 W m^{-2}, and 0.99, respectively. Thus, the H determined with each EC system was considered, in practice, to be identical. For data set_1, the slope, intercept, and R^2 comparing H_{EC} at $Z = 0.9$ m versus $Z = 1.5$ m were 0.93, -3 W m^{-2}, and 0.95, respectively, and the root mean square error, RMSE, was 11 W m^{-2}. For data set_2, the slope was 0.91, the intercept was 0 W m^{-2}, the R^2 was 0.98, and the RMSE was 9.5 W m^{-2}. In all, because the differences between the H measured at different heights were small, on average, within 6% and 10% for data set_1 and data set_2, respectively, the H used as a reference for comparison, H_{EC}, was determined by averaging the measured H at $Z = 0.9$ m and $Z = 1.5$ m.

3.3. Determination of the H Estimates

The canopy parameters d, z_{0m}, and kB^{-1} were estimated as $d = 2/3h$, $z_{0m} = 0.12h$, and $kB^{-1} = 2$ where h is the canopy height [*Garratt and Francey*, 1978; *Brutsaert*, 1982]. Regardless of the method applied to estimate H, the horizontal mean wind speed at height z is used as input in the wind log-law to estimate u_*. Two methods to estimate H will assume that $s_{(z)}$ remains constant under certain conditions, such as unstable or stable cases. Therefore, for a given Z, the constant value for $s_{(z)}$ was determined from equation (4) by forcing the linear regression through the origin. The stability case for each sample was discriminated by negative (stable) and positive (unstable) ramp dimensions.

3.3.1. Method $H_{Eq.(1)}$

Starting at neutral conditions, $z/L = 0$, the first estimate of u_* is obtained at z, which allows the first approximation of $r_{ah(z)}$ and $H_{Eq.(1)}$. The second approximation for z/L is then obtained and the process is repeated until convergence is achieved. The loop was stopped when the difference in u_* between two consecutive iterations, Δu_*, was $\Delta u_* \leq 0.005$ m s^{-1}. The method $H_{Eq.(1)}$ was applied to data set_1 and data set_2.

3.3.2. *Method* $H_{Eq.(10)}$

To solve equation (10), it was assumed that $s_{(z)}$ is known. Therefore, starting at neutral conditions, the first approach for coefficient a_2, equation (9), for z_{0h}, equation (8), and for u_*, wind log-law, were determined.

Table 1. Determination of Parameter $s_{(z)}$ for Data Set_1 and Data Set_2, for Each Measurement Height, Z (m), and Ramp Model[a]

Model	Z	$s_{(z)}$	R^2
Data Set_1 (N_{st} = 945)			
Chen	0.9	4.3	0.59
Chen	1.5	5.9	0.80
VA	0.9	5.0	0.49
VA	1.5	5.9	0.68
Data Set_2 (N_{st} = 132)			
Chen	0.9	1.9	0.55
Chen	1.5	1.7	0.57
VA	0.9	1.3	0.26
VA	1.5	1.6	0.25
Data Set_2 (N_{unst} = 289)			
Chen	0.9	2.7	0.58
Chen	1.5	2.5	0.68
VA	0.9	1.3	0.22
VA	1.5	1.7	0.21

[a] R^2 is the coefficient of determination, N is the number of samples, and subscripts, *unst* and *st*, denote unstable and stable cases, respectively.

Then, the first estimation of H, $H_{Eq.(10)}$, is obtained which allows calculation of the second approximation for z/L. Iterations were performed until they achieved $\Delta u_* \leq 0.005$ m s^{-1}. Two procedures were used to obtain $H_{Eq.(10)}$. One procedure, $H_{Eq.(10)snc}$, assumed that, for a given Z, the ramp dimensions were available every 0.5 h. Therefore, $s_{(z)}$ was determined for each sample. The other procedure, $H_{Eq.(10)sc}$, assumed that $s_{(z)}$ remains constant for unstable or stable cases. For practical purposes, when the VA's model was used in $H_{Eq.(10)sc}$, the ratio $\frac{(\tau - L_q)}{\tau}$ was assumed to be constant, otherwise a thermocouple operating at high frequency was still required. As a rule of thumb, $\frac{(\tau - L_q)}{\tau}$ was set to $\frac{(\tau - L_q)}{\tau} = 0.75$ [*Qiu et al.*, 1995; *Chen et al.*, 1997a]. The methods $H_{Eq.(10)nsc}$ and $H_{Eq.(10)sc}$ were used to estimate H for data set_1, but not for data set_2 because $\frac{\partial T_{(z)}}{\partial z}$ fell within the range of the measurement error.

3.3.3. Method $H_{Eq.(12)}$

It was assumed that $s_{(z)}$ remains constant for both unstable and stable cases. $H_{Eq.(12)}$ was determined using the Chen ramp amplitude. The parameter λ was set to $\lambda = 0.54$. Starting at neutral conditions, the first estimates of u_*, $\beta = \left(\frac{\lambda}{\pi k}\phi_{h(z/L)}\right)^{1/2}$, and H, equation (12), were obtained allowing for the next estimate of z/L. A loop was performed to achieve $\Delta u_* \leq 0.005$ m s^{-1}. The method $H_{Eq.(12)}$ was applied to data set_1 and data set_2.

4. Results

4.1. Performance of Parameter $s_{(z)}$

Table 1 shows for each data set, ramp model used, measurement height and stability conditions, the slope, $s_{(z)}$, and coefficient R^2 of the linear fitting forced through the origin of equation (4). Figure 2 shows $\left(T_c - T_{(z)}\right)$ versus $A_{(z)}$ determined using VA's model and the Chen's model for data set_1 at $Z = 0.9$ m, Figures 2a and 2b, respectively, and for data set_2 at $Z = 1.5$ m, Figures 2c and 2d, respectively. The corresponding figures for data set_1 at $Z = 1.5$ m were more highly correlated, while for data set_2 at $Z = 0.9$ m, the figures were similar. For data set_1, the linear trend is obvious, and $s_{(z)}$ was more scattered at $Z = 0.9$ m than at $Z = 1.5$ m and when VA's model was used. For data set_2, the scatter was larger than for data set_1 because $\left(T_c - T_{(z)}\right)$ may be small either under near-neutral or convective conditions that correspond to small and large ramp amplitudes, respectively. The latter is shown in Figures 2c and 2d, in order to avoid distorting the results of the linear regression, some of these samples (a total of 15 samples) were "by eye" classified as outliers and were, therefore, not included in Table 1. Even so, regardless of the measurement height and stability conditions, the values of R^2 given by VA's model were small. This issue suggests that the assumption that $s_{(z)}$ remains constant may only hold true for Chen's model when the gradients are small. All in all, on the basis of Figure 1, the observation of linear trends is not surprising for samples gathered under similar stability conditions. However, it is difficult to explain why Chen's model consistently better captured the variability of $\left(T_c - T_{(z)}\right)$ than VA's model. This issue is not intuitive. This is partly because a ramp model that takes the microfront period into account is more realistic than when it is neglected [*Chen et al.*, 1997a]. This issue requires further research over other canopies.

4.2. Performances of Equations (1), (10), and (12): The H Estimates

For each data set and measurement height, Table 2 shows the number of samples, the results of the linear regression analysis (slope, intercept, and coefficient R^2), the RMSE, and a coefficient D determined as the sum of the flux estimates $\left(\sum H_{Est}\right)$ over the sum of fluxes taken as a reference $\left(\sum H_{EC}\right)$, $D = \sum H_{Est} \Big/ \sum H_{EC}$. Because the linear regression analysis and the RMSE assumes that the independent variable is free of random errors, the coefficient D gives an integrated evaluation of the bias by averaging out random errors in the half-hourly estimates (i.e., the bias is $(D-1)$ times the mean value determined

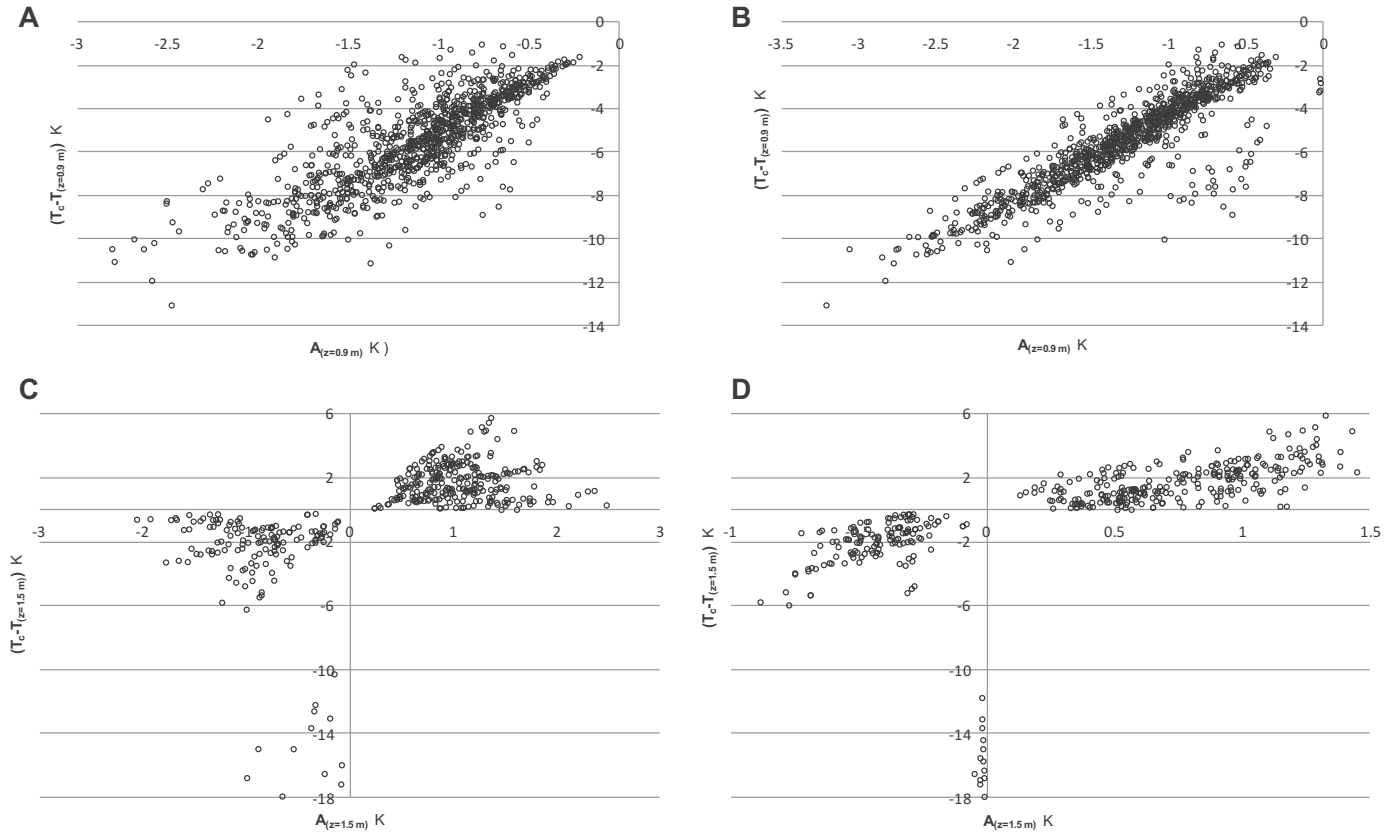

Figure 2. $(T_c - T_{(z)})$ versus $A_{(z)}$ determined for data set_1 at $Z = 0.9$ m using (a) VA's model and (b) Chen's model, and for data set_2 at $Z = 1.5$ m using (c) VA's model and (d) Chen's model.

from the observations). This is used to determine the percentage, p, being overestimated or underestimated, $p = 100 \cdot (1 - D)$ [*Mahrt*, 1988]. For all the data shown in Table 2, Figure 3 shows the estimates of H obtained at $Z = 1.5$ m using the traditional method, $H_{Eq.(1)}$, and methods $H_{Eq.(10)snc}$, $H_{Eq.(10)sc}$, and $H_{Eq.(12)}$ versus H_{EC}. The performance observed at $Z = 0.9$ m was similar.

4.2.1. Data Set_1

Regardless of Z and the method used to determine the H estimates, Table 2 shows that the slope and coefficient D were close because the intercepts were negligible (ranging from -6 to 10 W m^{-2}) and the correlations were, generally, high and similar; $0.74 \leq R^2 \leq 0.89$. However, while $H_{Eq.(1)}$ overestimated H_{EC} by about 70% and 50% at $Z = 0.9$ m and $Z = 1.5$ m, respectively, $H_{Eq.(10)snc}$ and $H_{Eq.(10)sc}$ using Chen's, and $H_{Eq.(12)}$ performed close to H_{EC} (i.e., within a 10% regardless of Z). It is difficult to explain why $H_{Eq.(10)snc}$ and $H_{Eq.(10)sc}$ using VA's model underestimated H_{EC} by about 60%. As a rule of thumb, a correction or enhancement factor, *ef*, of about 2 was required. Thus, to calculate the RMSE, the H estimates using VA's model were enhanced by setting, as a rule of thumb, $ef = 2$. In Table 2, these RMSE are shown in bold. In all, considering that the error in measuring H using different makes of triaxial sonic anemometers is in the order of 25 W m^{-2} (using the same postprocessing data protocol and same deployment height) and that in the experiment the two EC systems deployed at $Z = 0.9$ m and Z = 1.5 show a mean difference of 11 W m^{-2}, the H estimates using Chen's model were excellent, especially those showing D around 1.10 [*Mauder et al.*, 2007; *Foken*, 2008; *Frank et al.*, 2013]. The method $H_{Eq.(1)}$ was calibrated and the optimum kB^{-1} that fit H_{EC} was $kB^{-1} = 4.0$ and $kB^{-1} = 3.8$ at $Z = 0.9$ m and $Z = 1.5$ m, respectively. These kB^{-1} values minimized the RMSE, giving RMSE = 13 W m^{-2} and RMSE = 12 W m^{-2}, at $Z = 0.9$ m and $Z = 1.5$ m, respectively. When $s_{(z)}$ remains constant (i.e., observed by plotting $(T_c - T_{(z)})$ versus $A_{(z)}$), one could recommend the method $H_{Eq.(10)sc}$ using Chen's model because it is free of correction factors and the number of semiempirical parameters involved is smaller than using the $H_{Eq.(12)}$ method. However, to determine the coefficient a_2, the mean

Table 2. Comparison of the H Estimates Versus H_{EC} for Data Set_1 and Data Set_2[a]

Method	Z	s	int	R^2	RMSE	D
Data Set_1 (N = 945)						
$H_{Eq.(1)}$	0.9	1.71	−2	0.88	66	1.73
$H_{Eq.(1)}$	1.5	1.59	6	0.85	52	1.52
$H_{Eq.(10)snc}$ Chen	0.9	1.21	10	0.89	20	1.10
$H_{Eq.(10)snc}$ Chen	1.5	1.03	3	0.79	23	0.99
*H*Eq.(10)sc Chen	0.9	1.01	9	0.84	20	0.91
*H*Eq.(10)sc Chen	1.5	0.98	6	0.86	18	0.91
$H_{Eq.(10)snc}$ VA	0.9	0.30	−5	0.74	**30**	0.34
$H_{Eq.(10)snc}$ VA	1.5	0.33	−3	0.75	**31**	0.35
$H_{Eq.(10)sc}$ VA	0.9	0.41	1	0.88	**21**	0.40
$H_{Eq.(10)sc}$ VA	1.5	0.48	1	0.88	**15**	0.47
$H_{Eq.(12)}$ Chen	0.9	1.12	−3	0.89	21	1.10
$H_{Eq.(12)}$ Chen	1.5	0.91	−4	0.74	23	0.95
Data Set_2 (N = 421)						
$H_{Eq.(1)}$	0.9	1.04	−10	0.79	21	0.90
$H_{Eq.(1)}$	1.5	0.97	−9	0.80	19	0.83
$H_{Eq.(12)}$	0.9	0.90	−5	0.73	21	0.81
$H_{Eq.(12)}$	1.5	1.12	2	0.74	22	1.08

[a]N is the number of samples, Z (m) is the measurement height above the ground, s, int (W m^{-2}), and R^2 are the slope, intercept, and coefficient of determination of the linear regression analysis, respectively, RMSE (W m^{-2}) is the root mean square error, and D is the integrated H estimates over H_{EC}. The RMSE in bold denotes that the H estimates were enhanced by a factor of 2.

temperature must be available at two heights. Therefore, in practice, $H_{Eq.(12)}$ is very convenient and it is of interest to recall that the λ value used was obtained over straw mulch [*Chen et al*., 1997b].

4.2.2. The Data Set_2

Table 2 and Figures 3a and 3d show that $H_{Eq.(1)}$ and $H_{Eq.(12)}$ values were similar to H_{EC} except for some samples gathered under stable conditions. Regardless, in all cases, RMSE $\leq$ 22 W m^{-2} and calibration was not required for this data set.

4.3. Considerations Regarding Parameters $s_{(z)}$ and kB^{-1}

According to equation (8), z_{0h} depends on $s_{(z)}$ and coefficient a_2 which implies that kB^{-1} depends on stability conditions and on the momentum transferred to the ground. The latter agrees with *Brutsaert* [1982] who summarized previous works on kB^{-1} and concluded that it may depend on the roughness Reynolds number for aerodynamically smooth and bluff-rough surfaces, and also on the leaf area index and canopy structure for permeable roughness. In particular, equation (12) is similar to the approach obtained from equations (1) and (2) and assuming that kB^{-1} is constant, $H=\gamma u_*\left(T_c-T_{(z)}\right)$ where γ is a parameter that depends on the range observed for the stability parameter [*Kustas et al*., 1989]. This suggests that, to assume kB^{-1} constant, $s_{(z)}$ must perform fairly constant. This issue was observed in this study because for equation (4). Table 1 shows that using Chen's model, the correlations were relatively high, and Table 2 shows that the correlation between the traditional method, $H_{Eq.(1)}$ and H_{EC}, was excellent. Further research is required because $H_{Eq.(12)}$ and $H_{Eq.(1)}$ require the same input. However, as shown in Figure 2, it is straightforward to check when $s_{(z)}$ remains fairly constant.

At near-neutral conditions ($z/L \approx -0.002$ at $z = 5h$), from a wind tunnel experiment [*Böhm*, 2000] in which passive heat was emitted from both the underlying ground surface and canopy elements of a three-dimensional regular bluff-body array, *Haverd et al*. [2010] found that the resistance to heat transfer across the quasi-laminar boundary layer at the ground, r_{bg}, is related to flat-plate theory by implementing a factor, f_{SR}, that was $f_{SR} = 0.62$. The resistance at the ground was parameterized as, $r_{bg}=\frac{f_{SR}\delta_g}{\kappa_H}$, where f_{SR} corrects the value of one to account for surface renewal driven by intermittent large-scale eddies, κ_H is the molecular diffusivity and δ_g is the depth of the boundary layer of the ground that was defined as the height at which the molecular and turbulent diffusivities are equal. Thus, with $\delta_g=\frac{\kappa_H}{ku_{*g}}$ where u_{*g} is the friction velocity at the ground, $r_{bg}=\frac{f_{SR}}{ku_{*g}}$. Noteworthy to mention that $f_{SR} = 0.62$ was found to be independent on source heat distribution. The latter assessed by changing the heat flux partitioning across the canopy top, $H=H_g+H_c$ where subscripts g and c denote ground and canopy, respectively. Consequently, $f_{SR} = 0.62$ hold even for a highly tridimensional turbulent flow. For a flat-plate heat source (in practice, bare soils), H_g can be determined using bulk transfer formulation as, $\frac{H_g}{\rho C_p}=\frac{T_g-T_{\delta g}}{r_{bg}}$ where T_g and $T_{\delta g}$ are the temperatures measured

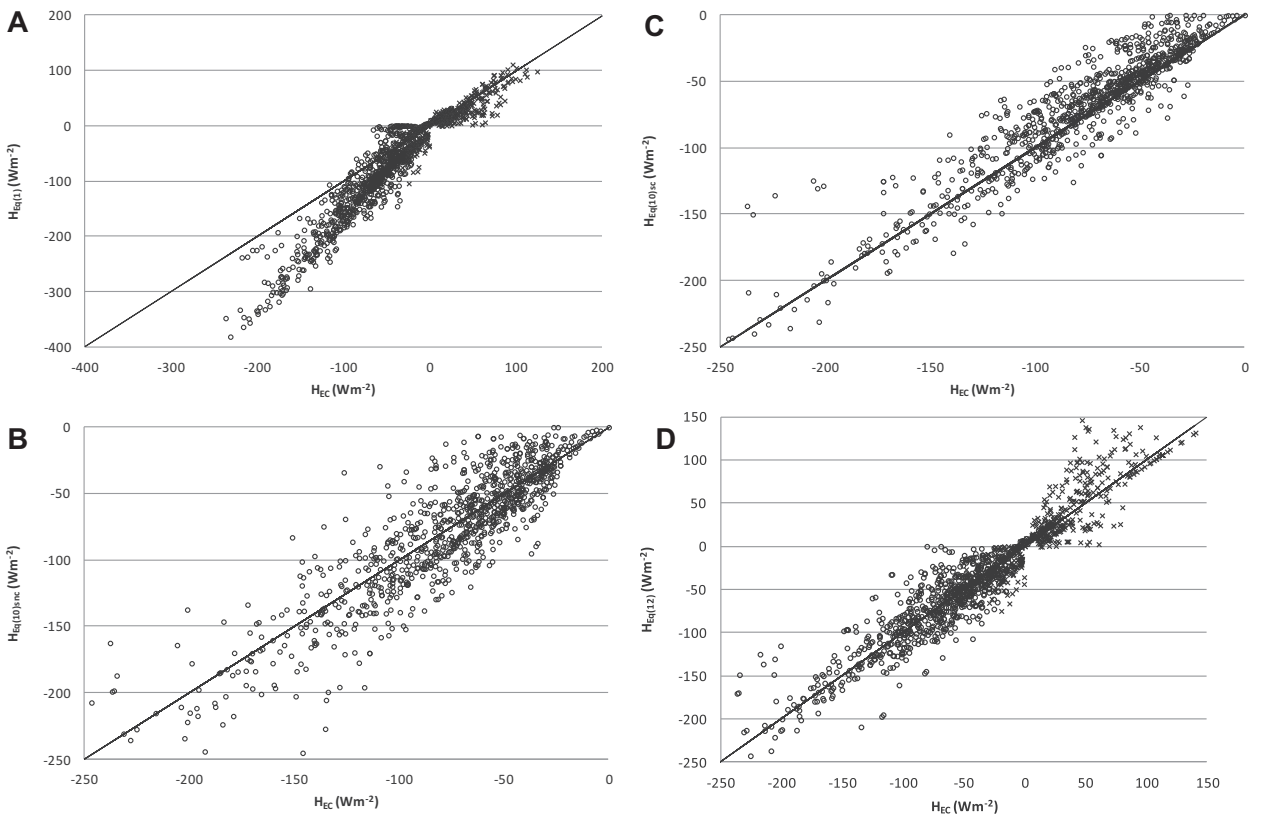

Figure 3. Sensible heat flux estimates (open circles and crosses for data set_1 and data set_2, respectively) determined at $Z = 1.5$ m versus H_{EC}. The H estimates were determined using the traditional method, (a) $H_{Eq.(1)}$, and methods, (b) $H_{Eq.(10)snc}$, (c) $H_{Eq.(10)sc}$, and (d) $H_{Eq.(12)}$, using the Chen's model.

ground level and at height δ_g, respectively. Alternatively, because there is evidence that coherent structures played a role in the heat transfer, H_g can also be determined in the framework of SR. In fact, near-neutral conditions equation (12) is recovered implementing equation (4) and $r_{bg} = \frac{f_{SR}}{k u_{*g}}$ in H_g, $\frac{H_g}{\rho C_p} = \frac{T_g - T_{\delta_g}}{r_{bg}} = \frac{k}{f_{SR}} u_{*g} A_{\delta_g} s_{\delta_g}$. Under the assumption that at near-neutral conditions, the parameter $k\beta$ at height δ_g was about $k\beta \approx 0.2$, which corresponds to measurements taken over bare soil at height Z = 0.03 m (over other canopies $k\beta \approx 0.25$ [*Castellví*, 2004]), it leads to $s_{\delta_g} \approx 0.2 \frac{f_{SR}}{k} = 0.3$. In practice, because determination of A_{δ_g} is difficult it may be recommended to use equation (8) for its estimation. By assuming $z_{0h} \approx \delta_g$ as rule of thumb, $A_\delta \approx A_{(z)} \left(1 + \frac{s_{(z)}}{f}\right)$. Because in sparse vegetation, H_g is dominant and required to apply two-source bulk transfer models, analysis on the performance of $s_{(z)}$ over bare soils and heterogeneous canopies may be valuable. Current research (not published) shows that taking measurements in the roughness sublayer (RSL) over a heterogeneous canopy (olive grove), $s_{(z)}$ is also fairly constant. The latter is interesting because the turbulence is more coherent than that in the inertial sublayer [*Finnigan et al.*, 2009] and, therefore, the natural sublayer to apply equation (12). Traditionally, to partition the sum $H_g + H_c$ into separate H_g and H_c has been done by means of surface resistance schemes [*Raupach and Finnigan*, 1995], thus equation (12) may offer alternative formulation.

5. Summary and Concluding Remarks

Because the bulk transfer formulation and SR analysis scale H with $u_* \left(T_c - T_{(z)}\right)$ and $u_* A_{(z)}$, respectively, we used the ratio, $s_{(z)}$, between $\left(T_c - T_{(z)}\right)$ and $A_{(z)}$ to estimate H avoiding the parameter kB^{-1} as input. It was found that $A_{(z)}$ determined using Chen's model better captured the variability of $\left(T_c - T_{(z)}\right)$ than the VA's model. Three methods to estimate H were proposed and tested. One assumed the need to determine $s_{(z)}$ half hourly, and the other two assumed that $s_{(z)}$ is, in practice, constant for a given range of stability conditions, such as unstable and stable cases. Obviously, each method requires different inputs; however, they

performed similarly well because $s_{(z)}$ was fairly constant throughout the experiment. Though further research is required, this issue could be generalized to other experiments because one can expect $s_{(z)}$ to remain constant under similar stability conditions. Therefore, because the three methods performed close to the EC method, the one requiring less input, $H_{\text{Eq.(12)}}$, is the most convenient in practice. The traditional method based on the bulk transfer formulation, $H_{\text{Eq.(1)}}$, required kB^{-1} calibration for stable cases. After calibration (against the EC method), its performance was excellent and similar to $H_{\text{Eq.(12)}}$. It may be suggested that this issue was a consequence of $s_{(z)}$ remaining constant when kB^{-1} was constant. Once kB^{-1} and $s_{(z)}$ are known, $H_{\text{Eq.(1)}}$ and $H_{\text{Eq.(12)}}$ are directly comparable because their input requirements are identical. This experiment was carried out in a region where shortly after noon an inversion forms during summer. For, some samples, $\left(T_c - T_{(z)}\right)$ and H_{EC} had different signs. This is a shortcoming inherent in equations (1) and (12) that can be identified by measuring the air temperature at high frequency to determine the sign of the third-order structure function. Though research is required, results obtained in a wind tunnel experiment suggest that equation (12) could be useful over bare soil and multilayer canopy modeling.

This study concludes that over an irrigated homogeneous, short and dense canopy at a site influenced by the regional advection of sensible heat flux, the three methods proposed for estimating H are alternatives to the traditional method because they perform close to the EC method, avoid kB^{-1} which is difficult to parameterize, and their cost of application is comparable (i.e., thermocouples are affordable) or identical.

Appendix A: The Profile of the Ramp Amplitude

Above the canopy, the one-dimensional diffusion equation holds [*Fitzmaurice et al*., 2004; *Priestley*, 1959]:

$$\frac{\partial \overline{T}_{(z,t)}}{\partial t} = \frac{\partial}{\partial z}\left(K_{h_{(z,t)}} \frac{\partial \overline{T}_{(z,t)}}{\partial z}\right) \tag{A1}$$

where the over bar denotes the mean value over time, such as 0.5 h, t is time, z is the measurement height above the zero-plane displacement, and $K_{h(z,t)}$ is the turbulent eddy diffusivity for heat. In the following, $K_{h(z)}$ is assumed to scale with $(u_* z)$, where u_* is the friction velocity. The mean air temperature $\overline{T}$ can be expressed as, $\overline{T}_{(z)} = fA_{(z)} + \overline{T}_b$ where $f = \frac{1}{2}\frac{(\tau - L_q)}{\tau}$ or $f = \frac{1}{2}$ using the ramp models proposed by *Van Atta* [1977] or *Chen et al*. [1997a], respectively, A and τ are the mean ramp amplitude and period, L_q is the quiescent period, and $\overline{T_b}$ is the air temperature at the top of the coherent structure [*Castellví and Snyder*, 2009]. Above the canopy, ramp time phases and $\overline{T_b}$ are not dependent on z [*Paw U et al*., 2005], neutral conditions are met at the initial time of the ramp formation [*Chen et al*., 1997b; *Gao et al*., 1989] and after ramp analysis, statistically, mean values over time can be determined over the ramp period [*Castellví*, 2013; *Chen et al*., 1997a; *Van Atta*, 1977]. Because $\frac{z}{\tau}$ scales with u_* (or the wind speed) [*Chen et al*., 1997b; *Paw U et al*., 2005; *Shapland et al*., 2012], we propose the following scale for (τK_h), $\tau K_h = \alpha z^2$ where α is a constant to be determined half hourly that depends on the momentum transferred to the ground and on the stability conditions. Therefore, starting at neutral conditions (i.e., $A_{(z,t=0)} = 0$), $\frac{\partial A_{(z,t)}}{\partial t} = \frac{A_{(z)}}{\tau}$, and (A1) can be rewritten as Euler's differential equation

$$A_{(z)} = \frac{\partial}{\partial z}\left(\beta z^2 \frac{\partial A_{(z)}}{\partial z}\right) \tag{A2}$$

where $\beta = \alpha f$. Because $\beta > 0$, the solution of (A2) is $A_{(z)} = B_1 z^{p_1} + B_2 z^{p_2}$, where B_1 and B_2 are the constants and $p_1 > 0$ and $p_2 < 0$ are the real roots of the characteristic equation, $1 = \beta p(p+1)$. Because the ramp amplitude diminishes with height, it is proposed to set $B_1 = 0$.

Acknowledgments
The authors thank C. M. U. Neale for his cooperation in the field and sharing instrumentation, Antonio, Asun, Carla, and Tània who provided access to different facilities in Córdoba and Lleida, and the reviewers for their constructive comments. This research was funded by CERESS project AGL2011–30498 (Ministerio de Economía y Competitividad of Spain, cofunded FEDER), CGL2012–37416-C04-01 (Ministerio de Ciencia y Innovación of Spain), and CEI Iberus, 2014 (Proyecto financiado por el Ministerio de Educación en el marco del Programa Campus de Excelencia Internacional of Spain). To acquire the database used in this manuscript contact P. Gavilán.

References

Ballard, J. R., J. A. Smith, and G. G. Koenig (2004), Towards a high temporal frequency grass canopy thermal IR model for background signatures, *Proc SPIE*, *5431*, 251–259.

Belcher, S. E., I. N. Harman, and J. J. Finnigan (2012), The wind in the willows: Flows in forest canopies in complex terrain, *Annu. Rev. Fluid Mech.*, *44*, 479–504.

Böhm, M. (2000), The role of source distribution on scalar transfer within and above plant canopies, PhD thesis, the Australian National University, 318 pp., Canberra, Australia.

Boulet, G., A. Olioso, E. Ceschia, O. Marloie, B. Coudert, V. Rivalland, J. Chirouze, and G. Chehbouni (2012), An empirical expression to relate aerodynamic and surface temperatures for use within single-source energy balance models, *Agric. For. Meteorol.*, *161*, 148–155.

Brutsaert, W. (1982), *Evaporation Into the Atmosphere. Environmental Fluid Mechanics*, 299 pp., Kluwer Acad., Dordrecht, Netherlands.

Castellví, F. (2004), Combining surface renewal analysis and similarity theory: A new approach for estimating sensible heat flux, *Water Resour. Res.*, *40*, W05201, doi:10.1029/2003WR002677.
Castellví, F. (2013), A method for estimating the sensible heat flux in the inertial sub-layer from high-frequency air temperature and averaged gradient measurements, *Agric. For. Meteorol.*, *180*, 68–75.
Castellví, F., and R. L. Snyder (2009), Combining the dissipation method and surface renewal analysis to estimate scalar fluxes from the time traces over rangeland grass near Ione (California), *Hydrol. Processes*, *23*(6), 842–857.
Castellví, F., P. J. Perez, and M. Ibañez (2002), A method based on high-frequency temperature measurements to estimate sensible heat flux avoiding the height dependence, *Water Resour. Res.*, *38*(6), 1084, doi:10.1029/2001WR000486.
Chamberlain, A. C. (1968), Transport of gases to and from surfaces with bluff and wave-like roughness elements, *Q. J. R. Meteorol. Soc.*, *94*, 318–332.
Chehbouni, A., D. Lo Seen, E. G. Njoku, and B. Monteny (1996), Examination of the difference between radiometric and aerodynamic surface temperatures over sparsely vegetated surfaces, *Remote Sens. Environ.*, *58*, 177–186.
Chen, W., M. D. Novak, T. A. Black, and X. Lee (1997a), Coherent eddies and temperature structure functions for three contrasting surfaces. Part I. Ramp model with finite micro-front time, *Boundary-Layer Meteorol.*, *84*, 99–123.
Chen, W., M. D. Novak, T. A. Black, and X. Lee (1997b), Coherent eddies and temperature structure functions for three contrasting surfaces. Part II. Renewal model for sensible heat flux, *Boundary-Layer Meteorol.*, *84*, 125–147.
Choudhury, B. J., R. J. Reginato, and S. B. Idso (1986), An analysis of infrared temperature observations over wheat and calculation of latent heat flux, *Agric. For. Meteorol.*, *37*, 75–88.
Christen, A., F. Meier, and D. Scherer (2012), High-frequency fluctuations of surface temperatures in an urban environment, *Theor. Appl. Climatol.*, *108*, 301–324.
Colaizzi, P. D., S. R. Evett, T. A. Howell, and J. A. Tolk (2004), Comparison of aerodynamic and radiometric surface temperature using precision weighing lysimeters, in *Remote Sensing and Modeling of Ecosystems for Sustainability, Proceedings of the Society of Photo-Optical Instrumentation Engineers*, edited by W. Gao and D. R. Shaw, pp. 215–229, SPIE Int. Soc. of Opt. Eng., Bellingham, Wash.
Crago, R. D., and R. J. Qualls (2014), Use of land surface temperature to estimate surface energy fluxes: Contributions of Wilfried Brutsaert and collaborators, *Water Resour. Res.*, *50*, 3396–3408, doi:10.1002/2013WR015223.
Derksen, D. S. (1974), Thermal infrared pictures and the mapping of microclimate, *Neth. J. Agric. Sci.*, *22*, 119–132.
Duynkerke, P. G. (1992), The roughness length for heat and other vegetation parameters for a surface of short grass, *J. Appl. Meteorol.*, *31*, 579–586.
Finnigan, J. J., R. H. Shaw, and E. G. Patton (2009), Turbulence structure above a vegetation canopy, *J. Fluid Mech.*, *637*, 387–424.
Fitzmaurice, J., J. Wang, and R. L. Brass (2004), Sensible heat flux estimated from one-level air temperature near the land surface, *Geophys. Res. Lett.*, *31*, L07102, doi:10.1029/2003GL018452.
Foken, T. (2008), *Micrometeorology*, Springer, Germany.
Frank, J. M., W. J. Massman, and B. E. Ewers (2013), Underestimates of sensible heat flux due to vertical velocity measurement errors in non-orthogonal sonic anemometers, *Agric. For. Meteorol.*, *172*, 72–81.
French, A. N., et al. (2012), Estimation of surface energy fluxes using surface renewal and flux variance techniques over an advective irrigated agricultural site, *Adv. Water Resour.*, *50*, 91–105.
Gao, W., R. H. Shaw, and K. T. Paw U (1989), Observation of organized structure in turbulent-flow within and above a forest canopy, *Boundary-Layer Meteorol.*, *47*, 349–377.
Garai, A., and J. Kleissl (2011), Air and surface temperature coupling in the convective atmospheric boundary layer, *J. Atmos. Sci.*, *68*, 2945–2954, doi:10.1175/JAS-D-11-057.1.
Garai, A., E. Pardyjak, G. J. Steeneveld, and J. Kleissl (2013), Surface temperature and surface-layer turbulence in a convective boundary layer, *Boundary-Layer Meteorol.*, *148*, 51–72.
Garratt, J. R., and R. J. Francey (1978), Bulk characteristics of heat transfer in the unstable baroclinic atmospheric boundary layer, *Boundary-Layer Meteorol.*, *15*, 399–421.
Graefe, J. (2004), Roughness layer corrections with emphasis on SVAT model applications, *Agric. For. Meteorol.*, *124*, 237–251.
Harman, I. N., and J. J. Finnigan (2007), A simple unified theory for flow in the canopy and roughness sublayer, *Boundary-Layer Meteorol.*, *123*, 339–363.
Harman, I. N., and J. J. Finnigan (2008), Scalar concentration profiles in the canopy and roughness sublayer, *Boundary-Layer Meteorol.*, *129*, 323–351.
Haverd, V., M. Böhm, and M. R. Raupach (2010), The effect of source distribution on bulk scalar transfer between a rough land surface and the atmosphere, *Boundary-Layer Meteorol.*, *135*, 351–368.
Hernández-Ceballos, M. A., J. A. Adame, J. P. Bolívar, and B. A. De la Morena (2013), A mesoscale simulation of coastal circulation in the Guadalquivir valley (southwestern Iberian Peninsula) using the WRF-ARW model, *Atmos. Res.*, *24*, 1–20.
Holzer, M., and E. D. Siggia (1994), Turbulent mixing of a passive scalar, *Phys. Fluids*, *6*, 1820–1837.
Hong, J., J. Kim, and Y. H. Byun (2012), Uncertainty in carbon exchange modelling in a forest canopy due to kB−1 parametrizations, *Q. J. R. Meteorol. Soc.*, *138*(664), 699–706.
Kalma, J. D., and D. L. B. Jupp (1990), Estimating evaporation from pasture using infrared thermometry: Evaluation of a one-layer resistance model, *Agric. For. Meteorol.*, *51*(3–4), 223–246.
Kustas, W. P., B. J. Choudhury, M. S. Moran, R. J. Reginato, R. D. Jackson, L. W. Gay, and H. L. Weaver (1989), Determination of sensible heat flux over sparse canopy using thermal infrared data, *Agric. For. Meteorol.*, *44*, 197–216.
Kustas, W. P., M. C. Anderson, J. M. Norman, and F. Q. Li (2007), Utility of radiometric-aerodynamic temperature relations for heat flux estimation, *Boundary-Layer Meteorol.*, *122*(1), 167–187.
L'Homme, J. P., A. Chehbouni, and B. Monteny (2000), Sensible heat flux-radiometric surface temperature relationship over sparse vegetation: Parameterizing B-1, *Boundary-Layer Meteorol.*, *97*(3), 431–457.
Liu, S., L. Lu, D. Mao, and L. Jia (2006), Measurement and estimation of the aerodynamic resistance, *Hydrol. Earth Syst. Sci. Discuss.*, *3*, 681–705.
Mahrt, L., and D. Vickers (2004), Bulk formulation of the surface heat flux, *Boundary-Layer Meteorol.*, *110*, 357–379.
Marth, L. (1988), Flux sampling errors for aircraft and towers, *J. Atmos. Oceanic Technol.*, *15*, 416–429.
Matsushima, D. (2005), Relations between aerodynamic parameters of heat transfer and 467 thermal-infrared thermometry in the bulk surface formulation, *J. Meteorol. Soc. Jpn.*, *83*(3), 373–389.
Mauder, M., S. P. Oncley, R. Vogt, T. Weidinger, L. Ribeiro, C. Bernhofer, T. Foken, W. Kohsiek, and H. Liu (2007), The energy balance experiment EBEX-2000, Part II: Inter-comparison of eddy-covariance sensors and post-field data processing methods, *Boundary-Layer Meteorol.*, *123*, 29–54.

McNaughton, K. G., and B. J. J. M. Van den Hurk (1995), A Lagrangian revision of the resistors in the two-layer model for calculating the energy budget of a plant canopy, *Boundary-Layer Meteorol.*, *74*, 261–288.
Owen, P. R., and W. R. Thomson (1963), Heat transfer across rough surfaces, *J. Fluid Mech.*, *15*, 321–334.
Paw U, K. T., Y. Brunet, S. Collineau, R. H. Shaw, T. Maitani, J. Qiu, and L. Hipps (1992), Evidence of turbulent coherent structures in and above agricultural plant canopies, *Agric. For. Meteorol.*, *61*, 55–68.
Paw U, K. T., J. Qiu, H.-B. Su, T. Watanabe, and Y. Brunet (1995), Surface renewal analysis: A new method to obtain scalar fluxes without velocity data, *Agric. For. Meteorol.*, *74*, 119–137.
Paw U, K. T., R. L. Snyder, D. Spano, and H.-B. Su (2005), Surface renewal estimates of scalar exchange, in *Micrometeorology in Agricultural Systems, Agron. Monogr.*, vol. 47, edited by J. L. Hatfield and J. M. Baker, pp. 455–483, ASA-CSSA-SSSA Publishers, Madison, Wis.
Priestley, C. H. B. (1959), *Turbulent Transfer in the Lower Atmosphere*, Univ. of Chicago Press, Chicago, Ill.
Qiu, J., K. T. Paw U, and R. H. Shaw (1995), Pseudo-wavelet analysis of turbulence patterns in three vegetation layers, *Boundary-Layer Meteorol.*, *72*, 177–204.
Raupach, M. R., and J. J. Finnigan (1995), Scale issues in boundary-layer meteorology: Surface energy balances in heterogeneous terrain, *Hydrol. Processes*, *9*, 589–612.
Schols, J. L. J., A. E. Jansen, and J. G. Krom (1985), Characteristics of turbulent structures in the unstable atmospheric surface layer, *Boundary-Layer Meteorol.*, *33*, 173–196.
Shapland, T. M., A. J. McElrone, R. L. Snyder, and K. T. Paw U (2012), Structure function analysis of two-scale scalar ramps. Part II: Ramp characteristics and surface renewal flux estimation, *Boundary-Layer Meteorol.*, *145*, 27–44.
Snyder, R. L., D. Spano, and K. T. Paw U (1995), Surface Renewal Analysis for sensible and Latent Heat Flux Density, *Boundary-Layer Meteorol.*, *77*, 249–266.
Steeneveld, G. J., B. J. H. Van de Wiel, and A. A. M. Holtslag (2006), Modelling the evolution of the atmospheric boundary layer coupled to the land surface for a three day period in CASES-99, *J. Atmos. Sci.*, *63*, 920–935.
Thom, A. S. (1975), Momentum, mass and heat exchange of plant communities, in *Vegetation and the Atmosphere*, edited by J. L. Monteith, pp. 57–109, Academic, London, U. K.
Troufleau, D., J. P. Lhomme, B. Monteny, and A. Vidal (1997), Sensible heat flux and radiometric surface temperature over sparse Sahelian vegetation. I. An experimental analysis of the kB-1 parameter, *J. Hydrol.*, *188–189*, 815–838.
Van Atta, C. W. (1977), Effect of coherent structures on structure functions of temperature in the atmospheric boundary layer, *Arch. Mech.*, *29*, 161–171.
Verhoef, A., H. A. R. de Bruin, and B. J. J. M. Van den Hurk (1997), Some practical notes on the parameter kB^{-1} for sparse vegetation, *J. Appl. Meteorol.*, *36*, 560–572.
Vogt, R. (2008), Visualisation of turbulent exchange using a thermal camera, in 18th Symposium on Boundary Layer and Turbulence, paper no. 8B.1, Stockholm, Sweden.
Yang, K., T. Koike, H. Ishikawa, J. Kim, X. Li, H. Z. Liu, S. M. Liu, Y. M. Ma, and J. M. Wang (2008), Turbulent flux transfer over bare-soil surfaces: Characteristics and parameterization, *J. Appl. Meteorol. Climatol.*, *47*(1), 276–290.